International Immunopharmacology 67 (2019) 231–238

Contents lists available at ScienceDirect

International Immunopharmacology

journal homepage: www.elsevier.com/locate/intimp

Effects of AT-RvD1 on paraquat-induced acute renal injury in mice

Xiao Hu, Yuanyuan Liang, Hongyu Zhao, Min Zhao*

Department of Emergency Medicine, Shengjing Hospital of China Medical University, Shenyang 110004, China

ARTICLE INFO

Keywords:
Paraquat
AT-RvD1
Acute renal injury

ABSTRACT

Objective: To investigate the effects of aspirin-triggered resolvin D1 (AT-RvD1) on paraquat-induced acute renal injury (ARI) in mice.

Methods: The ARI mouse model was established by administering 28 mg/kg paraquat to C57BL/6J mice by intraperitoneal injection. The mice received 10 or 100 ng AT-RvD1 by intravenous injection in the tail vein 2 h after toxication. The mice were euthanized 6, 24, or 72 h post-paraquat injection to collect blood and renal tissues. The samples were used to evaluate the pathological changes, renal function, inflammation and oxidative stress in the renal tissues.

Results: Compared with those of the PQ group, AT-RvD1 administration mitigated the pathological changes and improved renal function, activated Nrf2 and upregulated the expression of its downstream antioxidant genes (NQO1, HO-1, SOD1 and GPx1), and decreased the MDA and protein carbonyls content in renal tissues. Treatment also reduced the expression of P-selectin in renal tissues, the percentage of Ly-6G$^+$ CD41$^+$ cells in the peripheral blood and infiltration of neutrophils in renal tissues. Furthermore, AT-RvD1 inhibited the activation of NF-κB and reduced IL-1β and TNF-α serum levels.

Conclusion: The administration of AT-RvD1 can effectively suppress paraquat-induced oxidative stress injury and the inflammatory reaction, and alleviate paraquat-induced ARI.

1. Introduction

Paraquat is a bipyridyl quaternary ammonium salt herbicide that is extensively applied in the global agricultural field, especially in Asian countries due to its rapid action and lack of residue [1]. However, there is an dramatic increase of death cases caused by the suicide attempts or accidental exposure of paraquat in recent years. To date, there is no effective therapy against paraquat poisoning, and patient mortality is extremely high (up to 90%) [2]. Paraquat is mainly excreted by the kidneys in its original form. Thus, the kidneys are one of the organs with the highest concentration of this herbicide, which can explain the significant acute renal injury (ARI) occurring at an early stage of paraquat poisoning [3,4]. The proximal tubules are the primary site of paraquat damage and administration of paraquat to mice causes acute tubular degeneration and necrosis in the kidneys within 24 h [5]. These histopathological changes eventually lead to acute renal failure, which impairs the ability of the kidneys to further excrete paraquat. Clinically, paraquat toxicity presents as reduced glomerular filtration rate(GFR), albuminuria, and glycosuria. Ingestion of paraquat at doses > 20 mg/kg leads to acute tubular necrosis and renal failure in humans [6]. ARI seriously influences the excretion of paraquat and can cause a greater than five-fold increase in the paraquat plasma concentration. This increased concentration enhances the toxicity of paraquat, aggravates multiple organ dysfunction and significantly increase mortality [7,8]. Therefore, it is essential to treat paraquat poisoning to alleviate ARI and maintain renal function.

Although there are many studies about the mechanisms of paraquat poisoning, it has not been fully characterized. However, paraquat-induced redox cycling appears to be the foundation of paraquat toxicity. After entering the cell in the form of PQ^{2+}, PQ is reduced enzymatically by NADPH-cytochrome P-450 reductase to form the PQ^+ plus $NADP^+$. The PQ^+ is then rapidly reoxidized (returning to its original form PQ^{2+}) in the presence of O2 with subsequent generation of superoxide anions ($O_2^{\cdot-}$). PQ play a catalytic role in this redox cycling process, promoting the flow of electrons from NADPH to O2 and facilitating the production of O_2^- based on NADPH consumption [1]. The O_2^- contributes to a further cascade that induces the production of other reactive oxygen species (ROS), including H_2O_2 and ^-OH, which causes lipid peroxidation and cell injury [1]. In addition, numerous studies have shown that inflammation plays an important role in ARI and can cause persistent impairment of renal function [9,10]. ROS production and tissue injury can induce the infiltration of inflammatory cells and

* Corresponding author at: Department of Emergency Medicine, Shengjing Hospital of China Medical University, No. 36, Sanhao Street, Shenyang 110004, Liaoning Province, China.

E-mail address: zhaom@sj-hospital.org (M. Zhao).

https://doi.org/10.1016/j.intimp.2018.12.029
Received 20 November 2018; Received in revised form 9 December 2018; Accepted 11 December 2018
Available online 15 December 2018

the release of inflammatory cytokines [11,12]. Moreover, ROS and inflammatory cytokines can activate NF-κB and increase the expression of downstream pro-inflammatory genes, which enhances the inflammatory reaction [13]. Therefore, most therapies for paraquat poisoning focus on blocking the inflammation pathways or anti-oxidation. However, blocking a single pathway or target may not be effective because paraquat poisoning has a complex mechanism, and there may be several independent, but not mutually exclusive, mechanisms that jointly induce irreversible cell injury.

Recently, interest has increased in the role of endogenous lipid mediators derived from omega-3 polyunsaturated fatty acids (PUFAs) in resolving inflammation and promoting tissue homeostasis. Resolvin D1(RvD1) is generated by lipoxygenase from docosahexaenoic acid (DHA) [14]. It plays a significant role in abrogating inflammation in animal models of peritonitis [15], keratitis [16], and acute lung injury [17]. Using a mouse model of ischemia-reperfusion-induced ARI, Duffield et al. [18] demonstrated that the biological synthesis and release of RvD1 in renal tissues were significantly increased during ARI. Furthermore, supplementation with exogenous RvD1 could effectively improve the renal function of these mice. These data suggest that RvD1 is vital for the physiological regulation of the body against ARI. In the presence of aspirin, acetylated cyclooxygenase-2 (COX-2) catalyzes the conversion of DHA into aspirin triggered-resolvin D1 (AT-RvD1) [19], a 17R-epimer of RvD1. Although their mechanisms of action are similar, AT-RvD1 has greater activity and better stability in metabolic inactivation [19]. Chen et al. [20] found that AT-RvD1 had powerful anti-inflammatory properties in a mouse model of LPS-induced ARI, effectively inhibiting ARI. In addition, AT-RvD1 can effectively antagonize tissue injury via downregulation oxidative stress by Nrf2/KEAP1 pathway [21,22]. Therefore, we investigated whether AT-RvD1 could antagonize the nephrotoxicity caused by paraquat. In this study, we found that AT-RvD1 obviously suppressed paraquat-induced oxidative stress by activating Nrf2 and its downstream anti-oxidation genes, inhibited the interaction between neutrophils and platelets to reduce the infiltration of inflammatory cells in renal tissues, and regulated the expression of NF-κB and the release of inflammatory cytokines, thus effectively inhibiting paraquat-induced ARI.

2. Materials and methods

2.1. Animals

Male C57BL/6J mice (8 to 10 weeks, 18 to 22 g) were purchased from the Animal Center of China Medical University. The mice were housed in a standard laboratory environment (12 h/12 h light-dark cycle; temperature, 20 to 25 °C; relative humidity, 40 to 60%) with access to food and water ad libitum. The animal experiments were conducted following the animal experiment guidance principles of the Animal Ethics Committee of China Medical University.

2.2. Experimental plan

The mice (n = 18/group) were randomly divided into five groups: 1) control group, physiological saline intraperitoneally (IP) followed by intravenous (IV) physiological saline (tail vein) after 2 h; 2) AT-RvD1 group, physiological saline IP followed by 100 ng AT-RvD1 IV (tail vein) after 2 h; 3) paraquat group, 28 mg/kg paraquat IP followed by physiological saline IV (tail vein) after 2 h; 4) AT-RvD1-L group, 28 mg/kg paraquat IP followed by 10 ng AT-RvD1 IV (tail vein) after 2 h; 5) AT-RvD1-H group, 28 mg/kg paraquat IP followed by 100 ng AT-RvD1 IV (tail vein) after 2 h. Paraquat and AT-RvD1 were prepared in physiological saline and injected in a volume of 0.1 mL. At 6, 24, and 72 h post-paraquat toxication, six mice from each group were euthanized and the blood and kidneys were collected.

Both PQ and AT-RvD1 were diluted to 0.1 mL of physiological saline solution before use. The dose of PQ and AT-RvD1 was selected base on the previous literature [19,23]. PQ was obtained from Sigma-Aldrich (St. Louis, MO, USA) and AT-RvD1 was obtained from Cayman Chemical (Ann Arbor, MI, USA).

2.3. Detection of renal function

Blood samples were collected at 6, 24, and 72 h post-paraquat exposure and allowed to stand overnight at 4 °C and centrifuged at 10,000 rpm for 10 min to collect the serum. Creatinine and urea nitrogen serum levels were measured using a colorimetric kit (Sigma-Aldrich, St. Louis, MO, USA) according to the manufacturer's instructions.

2.4. Detection of IL-1β and TNF-α

Blood samples were collected at 6, 24, and 72 h post-paraquat exposure and allowed to stand overnight at 4 °C and centrifuged at 10,000 rpm for 10 min to collect the serum. IL-1β and TNF-α serum levels were detected using ELISA kits (R&D Systems, Minneapolis, MN, USA) according to the manufacturer's instructions.

2.5. Detection of MPO activity, MDA, GSH and protein carbonyls content in renal tissues

Renal tissues were collected at 6, 24, and 72 h post-paraquat exposure and processed into 10% homogenates and centrifuged to collect the supernatant. The myeloperoxidase (MPO) activity, malondialdehyde (MDA), reduced glutathione (GSH) and protein carbonyls content in the samples were measured using colorimetric (Sigma-Aldrich, St. Louis, MO, USA), TBARS (Sigma-Aldrich, St. Louis, MO, USA), spectrophotometric (Nanjing Jiancheng Bioengineering Institute, Nanjing, China) and colorimetric (Cayman Chemical, Ann Arbor, MI, USA) assay kits, respectively, according to the manufacturer's instructions.

2.6. Detection of SOD and GPx activities in renal tissues

Renal tissues were collected at 6, 24, and 72 h post-paraquat exposure and processed into 10% homogenates and centrifuged to collect the supernatant. Superoxide dismutase(SOD) and glutathione peroxidase (GPx) activities were assayed by using kits (Nanjing Jiancheng Bioengineering Institute, Nanjing, China) according to the manufacturer's instructions.

2.7. Detection of neutrophil and platelet interactions by flow cytometry

At 72 h after paraquat exposure, blood samples were prepared using RBC lysis buffer, blocked with the Fc of the CD16/32 antibody, and then incubated with Ly-6G (eBioScience, San Diego, CA, USA) and CD41 (eBioScience, San Diego, CA, USA) antibodies on ice for 20 min. The percentage of $Ly6G^+CD41^+$ cells was determined by flow cytometry.

2.8. Pathology of renal tissues

Renal tissues were collected at 72 h after paraquat exposure and fixed in 4% paraformaldehyde for 72 h, dehydrated with alcohol using a gradient of concentrations, embedded with paraffin, and cut into 4 μm sections. The sections were dewaxed and then stained with hematoxylin and eosin. The sections were analyzed for histopathological changes using light microscopy. The histopathological scoring for renal globular and tubular injury consisted of the following: 0, no injury; 1, < 10% injured cells; 2, 10 to 25% injured cells; 3, 25 to 40% injured cells; 4, 40 to 50% injured cells; 5, > 50% injured cells.

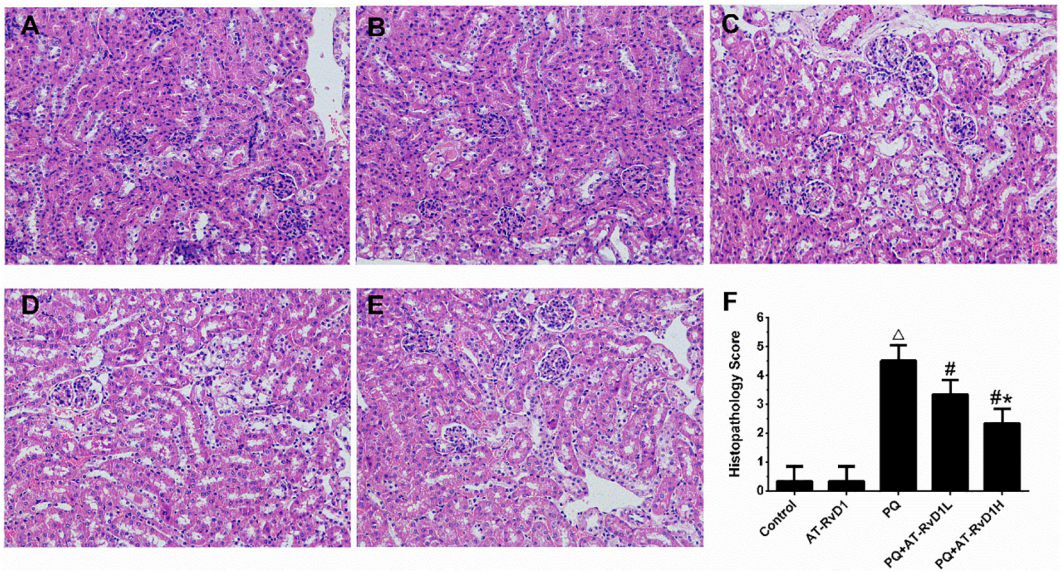

Fig. 1. AT-RvD1 attenuated PQ-induced histopathological changes. The renal histological changes were determined by HE staining(A-E) and histopathology score(F) at 72 h post PQ exposure. A:control group, B:AT-RvD1 group, C:PQ poisoning group, D: PQ poisoning + AT-RvD1 low dose group, E PQ poisoning + AT-RvD1 high dose group. AT-RvD1L: AT-RvD1 at low dose of 10 ng. AT-RvD1H: AT-RvD1 at high dose of 100 ng. $\triangle P < 0.05$ vs. control group, $\#P < 0.05$ vs. PQ group, $*P < 0.05$ vs. AT-RvD1L group (n = 6).

2.9. Western blotting

At 72 h after paraquat exposure, total protein, nuclear protein, and cytoplasmic protein were extracted from renal tissue homogenates using commercial kits (Beyotime Biotechnology, Shanghai,China). Equivalent amounts of protein samples were separated by 12% SDS-PAGE gel electrophoresis and transferred onto PVDF membranes. The blots were blocked with 5% skim milk for 1 h and then incubated with primary antibody (i.e., total NF-κB p65 (1:1000), phospho-NF-κB p65 (1:1000), P-selectin (1:4000), or Nrf2 (1:1000)) overnight at 4 °C. The blots were washed with TBST and then incubated with secondary antibody at room temperature for 1 h. The specific protein were visualized by ECL. Quantitative analysis was performed using Gel-Pro-Analyzer 6.3 software. β-actin was used as the total and cytoplasmic protein loading control and Lamin B served as the nuclear protein loading control. P-selectin antibody was purchased from Abcam (Cambridge, UK), and other antibodies were all bought from Cell Signaling Technology (Danvers, MA, USA).

2.10. qRT-PCR

At 72 h after paraquat exposure, RNA was extracted from renal tissue homogenates using Trizol reagent and then reverse transcribed into cDNA. PCR was performed using the cDNA as a template with the following primers:

NQO1 forward: 5′-GGTAGCGGCTCCATGTACTC-3′;
NQO1 reverse: 5′-CGCAGGATGCCACTCTGAAT-3′;
HO-1 forward: 5′-GCCCACCAAGTTCAAACAG-3′;
HO-1 reverse: 5′-GCTCCTCAAACAGCTCAATGT-3′;
SOD1 forward: 5′-GATCGTGTGATCTCACTCTC-3′;
SOD1 reverse: 5′-TTGTTTCTCATGGACCAC-3′;
GPx1 forward: 5′-CCCGTGCAATCAGTTC-3′;
GPx1 reverse: 5′-TTCGCACTTCTCAAACAA-3′;
β-actin forward: 5′-GGCTGTATTCCCCTCCATCG-3′;
β-actin reverse: 5′-CCAGTTGGTAACAATGCCATGT-3′. The qRT-PCR was performed using the Model 7500 Thermal Cycler (Applied Biosystems, Foster, CA, USA). All data were normalized to the fold of β-actin expression.

2.11. Immunofluorescence

Renal tissues were fixed in paraformaldehyde-lysine-periodate (PLP), soaked overnight in 20% sucrose-PBS solution, embedded with OCT (optimal cutting temperature) compound, frozen, and cut into 5-μm sagittal sections. The sections were blocked with 0.5% mouse BD Fc Block(San Jose, California, USA) in 3% FBS at room temperature for 30 min and immunolabelled with anti-Ly-6G antibody (1:200, eBioScience, San Diego, CA, USA), which was fluorescence-labeled with Cy3 (Beyotime Biotechnology, China). Samples were washed three times with PBS, mounted with ProLong Antifade Kit (Life technology, Grand Island, NY, USA), and observed by confocal fluorescence microscopy.

2.12. Statistical analysis

All data are presented as the mean ± standard deviation (mean ± SD). The multiple comparisons were performed using one-way ANOVA, respectively. $P < 0.05$ indicated a statistically significant difference.

3. Results

3.1. AT-RvD1 mitigated paraquat-induced ARI

HE staining of the renal tissues showed that the mice in both the control and AT-RvD1 groups had a normal kidney structure, including the renal globules and tubules, with regularly arranged epithelial cell nuclei in the renal tubules (Fig. 1A and B). In contrast, the renal tissue of the paraquat group displayed apparent edema, detachment and necrosis of epithelial cells, lumen dilation and distortion in the proximal convoluted renal tubules (Fig. 1C). AT-RvD1 treatment markedly mitigated paraquat-induced tubular injury mentioned above (Fig. 1D and E).

The renal function of mice was evaluated using the creatinine and urea nitrogen serum levels. Compared to the control group, the creatinine and urea nitrogen serum levels significantly increased after paraquat toxication, which was suppressed by AT-RvD1 (Fig. 2).

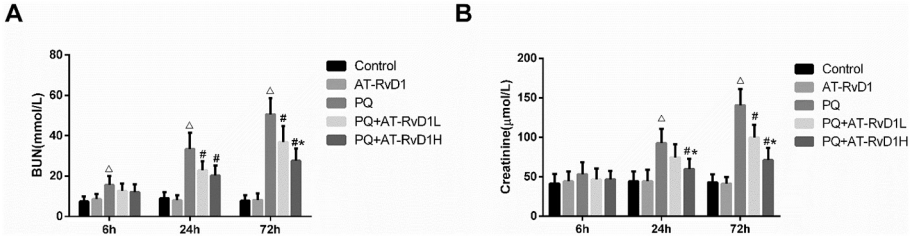

Fig. 2. AT-RvD1 alleviated PQ-induced renal impairment. At 6,24 and 72 h after PQ exposure, blood samples were collected for analysis of renal function. Serum BUN level(A) and Creatinine level(B) were significantly reduced by AT-RvD1 administration after PQ exposure. AT-RvD1L: AT-RvD1 at low dose of 10 ng. AT-RvD1H: AT-RvD1 at high dose of 100 ng. $\triangle P < 0.05$ vs. control group, $\#P < 0.05$ vs. PQ group, $*P < 0.05$ vs. AT-RvD1L group (n = 6).

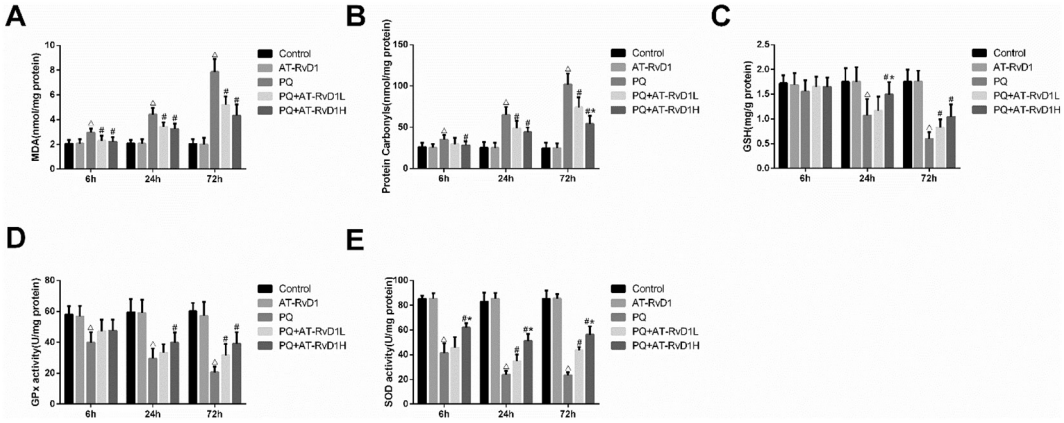

Fig. 3. The measurement of oxidative stress markers. At 6,24 and 72 h after PQ exposure, renal tissus were collected for analysis of MDA(A), protein carbonyls(B), GSH(C) levels and GPx(D) and SOD(E) activity. AT-RvD1L: AT-RvD1 at low dose of 10 ng. AT-RvD1H: AT-RvD1 at high dose of 100 ng. $\triangle P < 0.05$ vs. control group, $\#P < 0.05$ vs. PQ group, $*P < 0.05$ vs. AT-RvD1L group ($n = 6$).

3.2. AT-RvD1 reduced oxidative stress in renal tissues

The paraquat-induced oxidative stress in the renal tissues was evaluated by measuring the MDA, protein carbonyls and GSH content. The MDA and protein carbonyls content in the renal tissues was significantly higher in the paraquat group than in the control group. However, AT-RvD1 markedly decreased the MDA and protein carbonyls content (Fig. 3A and B). The levels of GSH in the renal tissues were significantly reduced in the PQ group compared with the control group. This effect was markedly reversed by AT-RvD1 (Fig. 3C).

We also measured SOD and GPx activity in renal tissues. PQ administration resulted in a significant decrease in enzyme activities of SOD and GPx. However, AT-RvD1 treatment counteracted these effects in a dose dependent manner (Fig. 3D and E).

To better understand the mechanism of the regulation of oxidative stress by AT-RvD1, we measured the expression of Nrf2 and its downstream target genes NADPH: quinone oxidoreductase-1 (NQO1), heme oxygenase-1 (HO-1), superoxide dismutase1 (SOD1) and glutathione peroxidase1 (GPx1). Compared to the control group, Nrf2 nuclear translocation was significantly reduced in the renal tissues from the paraquat group. However, AT-RvD1 upregulated the intranuclear expression of Nrf2 compared to the paraquat group (Fig. 4A and B). In addition, AT-RvD1 upregulated the mRNA expression of HO-1 (Fig. 4C), NQO1 (Fig. 4D), SOD1 (Fig. 4E) and GPx1(Fig. 4F), which further suggested that AT-RvD1 effectively activated the Nrf2 signaling pathway.

3.3. AT-RvD1 suppressed the release of inflammatory cytokines

The IL-1β and TNF-α serum levels were significantly higher in the paraquat group than in the control group, which were reduced by treatment with AT-RvD1(Fig. 5A and B). This finding suggested that AT-RvD1 could effectively inhibit the paraquat-induced release of inflammatory cytokines.

3.4. AT-RvD1 inhibited NF-κB activation

To further understand the molecular mechanism underlying the anti-inflammatory effects of AT-RvD1, NF-κB expression was measured in the renal tissues. The degree of NF-κB nuclear translocation in the paraquat group was significantly greater than in the control group. However, this translocation was reversed by AT-RvD(Fig. 6A and B).

3.5. AT-RvD1 decreased the infiltration of neutrophil in renal tissues

The infiltration of neutrophil in renal tissues was evaluated by immunofluorescence staining for Ly-6G (Fig. 7). Ly-6G staining were significantly higher in the paraquat group than in the control group. AT-RvD1 markedly inhibited the neutrophil infiltration induced by paraquat.

The detection of MPO activity further suggested that AT-RvD1 inhibited the infiltration of inflammatory cells into the renal tissues. Compared to the control group, paraquat resulted in a significant increase in MPO activity in the renal tissues, which decreased in response to AT-RvD1 (Fig. 5C).

3.6. AT-RvD1 inhibited the interaction between neutrophils and platelets

Neutrophils were labeled with a Ly-6G antibody and platelets with a CD41 antibody, and then the percentage of Ly-6G$^+$ CD41$^+$ cells was determined in the peripheral blood by flow cytometry to evaluate the interaction between neutrophils and platelets (Fig. 8). Compared to the paraquat group, the percentage of Ly-6G$^+$ CD41$^+$ cells in the AT-RvD1 treatment group was significantly decreased.

Because P-selectin plays an important role in the interaction between neutrophils and platelets and the activation of neutrophils [24], we determined the levels of P-selectin expression in the renal tissues. The results showed that AT-RvD1 caused a decrease in P-selectin expression compared to the paraquat group (Fig. 6C and D).

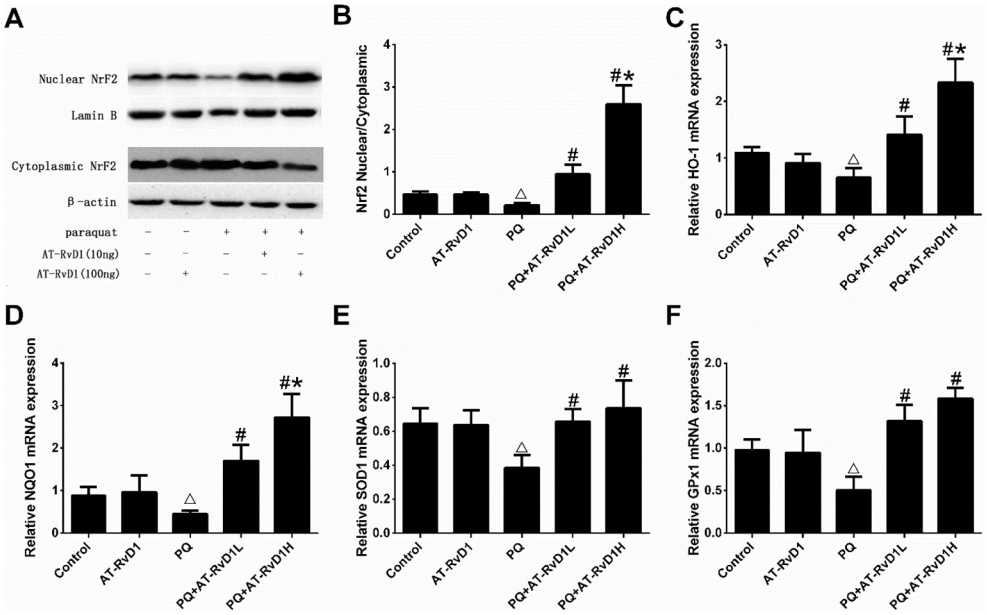

Fig. 4. AT-RvD1 activated the Nrf2 signaling pathway in the renal tissues. AT-RvD1 significantly promoted the nuclear translocation of Nrf2(A and B) and the mRNA expression of HO-1(C), NQO1(D), SOD1(E) and GPx1(F) after PQ exposure. The nuclear translocation of Nrf2 are presented as Nrf2 nuclear/cytoplasmic. The mRNA expression data are presented as fold change normalized to β-actin expression. AT-RvD1L: AT-RvD1 at low dose of 10 ng. AT-RvD1H: AT-RvD1 at hige dose of 100 ng. $\triangle P < 0.05$ vs. control group, $\#P < 0.05$ vs. PQ group, $*P < 0.05$ vs. AT-RvD1L group (n = 6).

4. Discussion

With its high morbidity and mortality, paraquat poisoning is becoming a public health issue. After entering into human body, 90% of the paraquat is excreted from the kidneys [3], and normal renal function is closely related to the plasma paraquat concentration and the severity of the damage to the organs [7]. Therefore, it is critical to maintain normal renal function in patients suffering from paraquat poisoning. In the present study, we found that paraquat could induce significant renal injury, including the epithelial cell detachment and necrosis, lumen dilation and distortion in the renal tubules. Renal function tests further confirmed the nephrotoxicity of paraquat. These findings demonstrate that paraquat is strongly nephrotoxic and can cause ARI in the early stages of poisoning. AT-RvD1 significantly reversed the nephrotoxicity of paraquat and alleviated ARI through the inhibition of oxidative stress, the reduction in the infiltration of inflammatory cells, and the suppression of neutrophil-platelet interactions, inflammatory cytokine release, and the inflammation signaling pathway.

Currently, the mechanism of paraquat-induced ARI has not been fully clarified, but it is widely accepted that paraquat-induced oxidative stress plays a key role in this process [1]. Paraquat can induce the production of massive levels of ROS by catalyzing a series of redox cycling. ROS can extract the hydrogen atoms from polyunsaturated fatty acids (PFA) constituting the cell membrane, thus breaking the integrity of the cell membrane and causing cell injury [25]. ROS can also add carbonyl groups to amino acid residues in proteins resulting in the oxidative inactivation of several key metabolic enzymes [1]. In this study, we determined the levels of oxidative stress in renal tissues by measuring the levels of MDA and protein carbonyls. The MDA and protein carbonyls content in the mouse renal tissues was significantly increased in the paraquat group, which was abrogated by the administration of AT-RvD1. These data suggest that AT-RvD1 can effectively inhibit paraquat-induced oxidative stress. To further clarify the molecular mechanism of AT-RvD1-mediated anti-oxidation, we measured Nrf2 expression in the renal tissues. Nrf2 plays an important role in the oxidation-antioxidation balance of the body by controlling the transcriptional activity of antioxidases downstream [26,27]. Under normal physiological conditions, Nrf2 mainly binds to its inhibitory protein Keap1 and exists in the cytoplasm in a non-active state. When cells are stimulated by ROS, Nrf2 and Keap1 are uncoupled, and activated Nrf2 is transported into the cell nucleus and forms a heterodimer with Maf. The heterodimer binds to the ARE to activate the transcription of downstream genes [28,29]. In the present study, AT-RvD1 significantly increased the nuclear translocation of Nrf2 and the expression of downstream antioxidases (NQO1, HO-1, SOD1 and GPx1), suggesting that AT-RvD1 suppresses paraquat-induced oxidative stress by regulating the Nrf2 signaling pathway. These findings increased our understanding of the bioactivity of AT-RvD1 and provided a new target and theoretical basis for potential clinical application.

Although the mechanism of ARI is still unclear, ARI is generally perceived as an inflammatory disease [30] with inflammatory renal injury a key factor in causing many progressive renal diseases [31,32]. Inflammatory cells, especially neutrophils, can release massive proteases, ROS, and cytokines. Therefore, they are considered major mediators of induced tissue injury [33]. According to previous studies, AT-RvD1 has a powerful inhibitory effect on leukocyte aggregation at the site of inflammation in models of mouse colitis [34], temporomandibular arthritis [7] and renal ischemia-reperfusion injury [18], which was also observed in our study. Indeed, Ly-6G staining was markedly reduced by AT-RvD1 treatment, which indicates that AT-RvD1 can effectively inhibit paraquat-induced neutrophil infiltration.

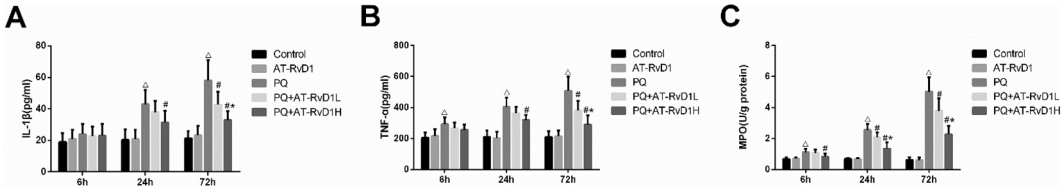

Fig. 5. AT-RvD1 inhibited the increase of L-1β and TNF-α levels in serum, and MPO activity in renal tissues after PQ exposure. At 6, 24 and 72 h after PQ exposure, blood samples and renal tissues were collected to measure the level of IL-1β(A) and TNF-α(B) in the serum, and MPO activity(C) in renal tissue. AT-RvD1L: AT-RvD1 at low dose of 10 ng. AT-RvD1H: AT-RvD1 at high dose of 100 ng. $\triangle P < 0.05$ vs. control group, $\#P < 0.05$ vs. PQ group, $*P < 0.05$ vs. AT-RvD1L group (n = 6).

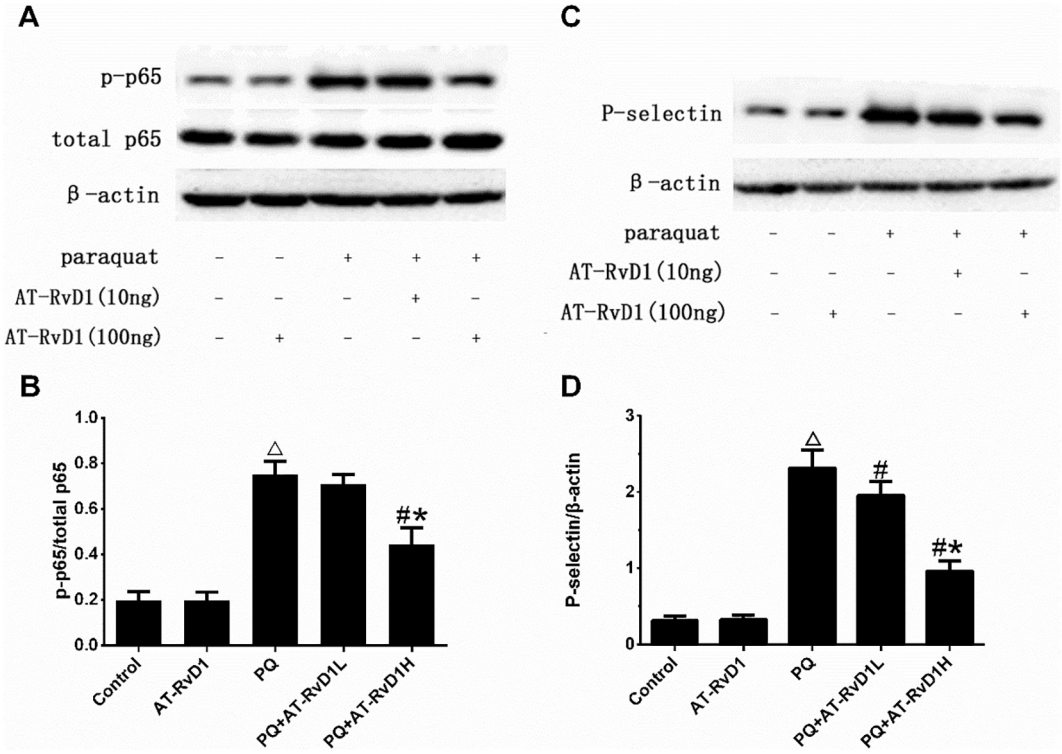

Fig. 6. The expression of NF-κB and P-Selectin in the renal tissue. AT-RvD1 markedly inhibited NF-κB activation(A and B) and downregulated P-Selectin expression(C and D). The nuclear translocation of NF-κB is presented as p-p65/total p65. AT-RvD1L: AT-RvD1 at low dose of 10 ng. AT-RvD1H: AT-RvD1 at high dose of 100 ng. $\triangle P < 0.05$ vs. control group, $\#P < 0.05$ vs. PQ group, $*P < 0.05$ vs. AT-RvD1L group ($n = 6$).

During neutrophil migration towards an inflammatory site, the adhesion molecule P-selectin can strengthen the interaction between neutrophils and platelets in the blood or adhering to the vascular endothelium. This interaction promotes the rolling and initial adhesion of neutrophils to the vascular endothelium, eventually leading to the abovementioned migration [35]. In this study, P-selectin expression in the renal tissues was significantly inhibited by AT-RvD1. Furthermore, AT-RvD1 caused a marked decrease in the number of Ly-6G$^+$ CD41$^+$ cells in the peripheral blood. These data suggest that AT-RvD1 suppressed the interaction between neutrophils and platelets by regulating P-selectin expression and reduced the activation and tissue infiltration of neutrophils.

AT-RvD1 not only inhibited the infiltration of leukocytes, but also effectively suppressed the release of inflammatory cytokines. As found in this study, there was a significant decline in the TNF-α and L-1β levels in the peripheral blood of paraquat-toxicated mice after the

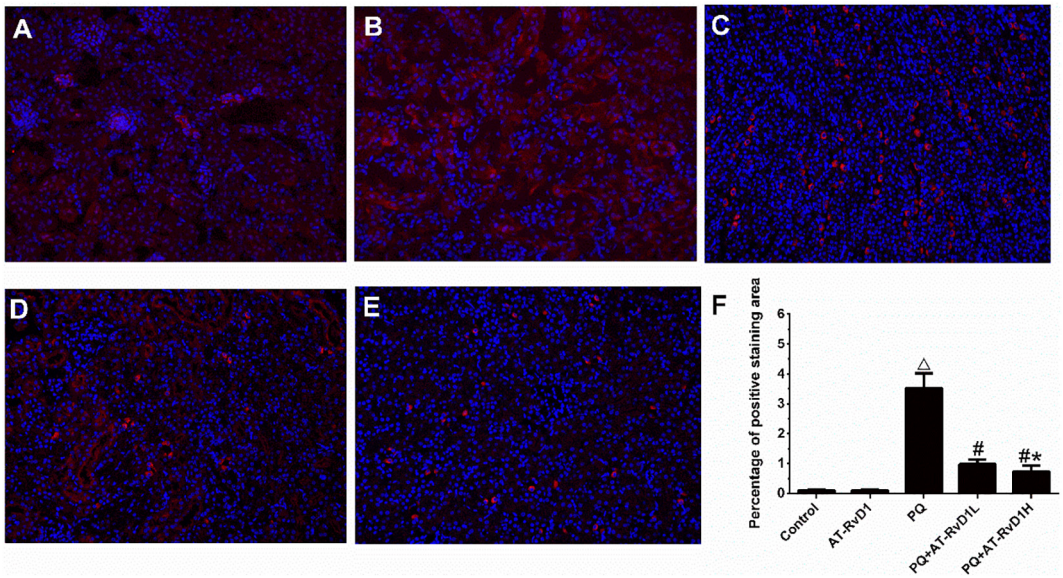

Fig. 7. AT-RvD1 reduced neutrophil infiltration in the renal tissue. The infiltration of neutrophil in renal tissues was evaluated by immunofluorescence staining for Ly-6G. A:control group, B:AT-RvD1 group, C:PQ poisoning group, D: PQ poisoning + AT-RvD1 low dose group, E PQ poisoning + AT-RvD1 high dose group. AT-RvD1L: AT-RvD1 at low dose of 10 ng. AT-RvD1H: AT-RvD1 at high dose of 100 ng. $\triangle P < 0.05$ vs. control group, $\#P < 0.05$ vs. PQ group, $*P < 0.05$ vs. AT-RvD1L group (n = 6).

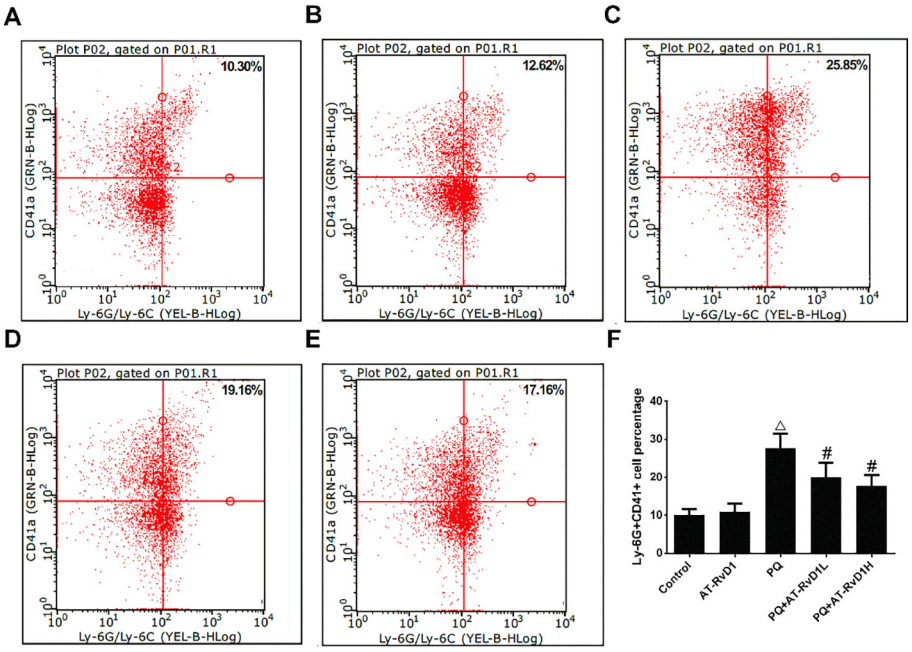

Fig. 8. AT-RvD1 inhibited the platelet–neutrophil interactions. Cell-cell interactions between PMNs and platelets were monitored by flow cytometry. The percentages of Ly-6G+ CD41+ cells are indicated at the top of the respective gates. A:control group, B:AT-RvD1group, C:PQ poisoning group, D: PQ poisoning + AT-RvD1 low dose group, E PQ poisoning+ AT-RvD1 high dose group. AT-RvD1L: AT-RvD1 at low dose of 10 ng. AT-RvD1H: AT-RvD1 at high dose of 100 ng. $\triangle P < 0.05$ vs. control group, $\#P < 0.05$ vs. PQ group, $*P < 0.05$ vs. AT-RvD1L group (n = 6).

administration of AT-RvD1. Such an effect was correlated with the inhibitory effect of AT-RvD1 on NF-κB activation [34,36]. When NF-κB binds to inhibitor κB (IκB), it exists as an inactive form located in the cytoplasm [37]. Cytokines, ROS, and endotoxin induce the rapid phosphorylation, ubiquitination, and fast degradation of IκB. This process activates NF-κB, which enters the nucleus and binds to the κB unit on DNA to regulate the transcription of downstream target genes, including inflammatory cytokines, chemotactic factors, and adhesion molecules, which amplifies the signaling cascade and the diffusion of the inflammatory reaction [38]. In the present study, our results demonstrated that AT-RvD1 significantly inhibited the nuclear translocation of NF-κB, which indicates that AT-RvD1 could effectively suppress the activation of NF-κB signaling pathway. Oxidative stress and inflammatory response are not independent but promote each other. ROS can activate NF-κB to induce the release of inflammatory factors and infiltration of inflammatory cells, while inflammatory cells can release large amounts of ROS to enhance local oxidative stress. This experiment demonstrates that AT-RvD1 simultaneously blocks the oxidative stress and inflammatory response induced by paraquat by multiple pathways, and thus has a strong antagonistic effect on paraquat nephrotoxicity.

In conclusion, this study demonstrated that AT-RvD1 could effectively antagonize the nephrotoxicity mediated by paraquat poisoning and mitigate paraquat-induced ARI. This effect is achieved through a variety of ways, including inhibition of oxidative stress by activating Nrf2 and its downstream anti-oxidation genes, blocking of inflammatory responses by inhibiting the nuclear translocation of NF-κB and the release of inflammatory cytokines, and suppression of the interaction between neutrophils and platelets. It's the first time to report that AT-RvD1 suppressed paraquat-induced oxidative stress by activating Nrf2 and its downstream anti-oxidation genes in renal tissue. This study provided a better understanding of the bioactivity of AT-RvD1 and suggests that the activation of the endogenous AT-RvD1 synthesis pathway or supplementation with exogenous AT-RvD1 may help alleviate paraquat-induced ARI. Thus, AT-RvD1 may represent a potential new target for the clinical treatment of paraquat poisoning.

Conflict of interest

The authors declare that there are no conflicts of interest.

Acknowledgements

This work was supported by Science Foundation of Liaoning Education Department [grant numbers LK201633, LK201603]; the Provincial Natural Science Foundation of Liaoning [grant numbers 201602879].

References

[1] R.J. Dinis-Oliveira, J.A. Duarte, A. Sanchez-Navarro, F. Remiao, M.L. Bastos, F. Carvalho, Paraquat poisonings: mechanisms of lung toxicity, clinical features, and treatment, Crit. Rev. Toxicol. 38 (2008) 13–71.
[2] H.J. Yu, Q. Fang, [Clinical data analysis of severe acute paraquat poisoning]. Zhonghua lao dong wei sheng zhi ye bing za zhi, Chin. J. Ind. Hyg. Occup. Dis. 28 (2010) 786–787.
[3] R.E. Murray, J.E. Gibson, A comparative study of paraquat intoxication in rats, guinea pigs and monkeys, Exp. Mol. Pathol. 17 (1972) 317–325.
[4] C.W. Sharp, A. Ottolenghi, H.S. Posner, Correlation of paraquat toxicity with tissue concentrations and weight loss of the rat, Toxicol. Appl. Pharmacol. 22 (1972) 241–251.
[5] J.L. Ecker, J.B. Hook, J.E. Gibson, Nephrotoxicity of paraquat in mice, Toxicol. Appl. Pharmacol. 34 (1975) 178–186.
[6] J.A. Vale, T.J. Meredith, B.M. Buckley, Paraquat poisoning: clinical features and immediate general management, Hum. Toxicol. 6 (1987) 41–47.
[7] M.S. Rose, E.A. Lock, L.L. Smith, I. Wyatt, Paraquat accumulation: tissue and species specificity, Biochem. Pharmacol. 25 (1976) 419–423.
[8] C. Bismuth, J.M. Scherrmann, R. Garnier, F.J. Baud, P.G. Pontal, Elimination of paraquat, Hum. Toxicol. 6 (1987) 63–67.
[9] S.N. Heyman, W. Lieberthal, P. Rogiers, J.V. Bonventre, Animal models of acute tubular necrosis, Curr. Opin. Crit. Care 8 (2002) 526–534.
[10] J.V. Bonventre, A. Zuk, Ischemic acute renal failure: an inflammatory disease? Kidney Int. 66 (2004) 480–485.
[11] A.M. Molck, C. Friis, The cytotoxic effect of paraquat to isolated renal proximal tubular segments from rabbits, Toxicology 122 (1997) 123–132.
[12] X. Wang, F. Luo, H. Zhao, Paraquat-induced reactive oxygen species inhibit neutrophil apoptosis via a p38 MAPK/NF-kappaB-IL-6/TNF-alpha positive-feedback circuit, PLoS One 9 (2014) e93837.
[13] M.H. Park, J.T. Hong, Roles of NF-kappaB in cancer and inflammatory diseases and their therapeutic approaches, Cell 5 (2016).
[14] C.N. Serhan, S. Hong, K. Gronert, S.P. Colgan, P.R. Devchand, G. Mirick, et al., Resolvins: a family of bioactive products of omega-3 fatty acid transformation circuits initiated by aspirin treatment that counter proinflammation signals, J. Exp. Med. 196 (2002) 1025–1037.
[15] L.V. Norling, J. Dalli, R.J. Flower, C.N. Serhan, M. Perretti, Resolvin D1 limits polymorphonuclear leukocyte recruitment to inflammatory loci: receptor-dependent actions, Arterioscler. Thromb. Vasc. Biol. 32 (2012) 1970–1978.
[16] Y. Jin, M. Arita, Q. Zhang, D.R. Saban, S.K. Chauhan, N. Chiang, et al., Anti-angiogenesis effect of the novel anti-inflammatory and pro-resolving lipid mediators, Invest. Ophthalmol. Vis. Sci. 50 (2009) 4743–4752.
[17] B. Wang, X. Gong, J.Y. Wan, L. Zhang, Z. Zhang, H.Z. Li, et al., Resolvin D1 protects

mice from LPS-induced acute lung injury, Pulm. Pharmacol. Ther. 24 (2011) 434–441.
[18] J.S. Duffield, S. Hong, V.S. Vaidya, Y. Lu, G. Fredman, C.N. Serhan, et al., Resolvin D series and protectin D1 mitigate acute kidney injury, J. Immunol. 177 (2006) 5902–5911.
[19] Y.P. Sun, S.F. Oh, J. Uddin, R. Yang, K. Gotlinger, E. Campbell, et al., Resolvin D1 and its aspirin-triggered 17R epimer. Stereochemical assignments, anti-inflammatory properties, and enzymatic inactivation, J. Biol. Chem. 282 (2007) 9323–9334.
[20] J. Chen, S. Shetty, P. Zhang, R. Gao, Y. Hu, S. Wang, et al., Aspirin-triggered resolvin D1 down-regulates inflammatory responses and protects against endotoxin-induced acute kidney injury, Toxicol. Appl. Pharmacol. 277 (2014) 118–123.
[21] R. Cox Jr., O. Phillips, J. Fukumoto, I. Fukumoto, P.T. Parthasarathy, S. Arias, et al., Enhanced resolution of hyperoxic acute lung injury as a result of aspirin triggered resolvin D1 treatment, Am. J. Respir. Cell Mol. Biol. 53 (2015) 422–435.
[22] S.V. Posso, N. Quesnot, J.A. Moraes, L. Brito-Gitirana, E. Kennedy-Feitosa, M.V. Barroso, et al., AT-RVD1 repairs mouse lung after cigarette smoke-induced emphysema via downregulation of oxidative stress by NRF2/KEAP1 pathway, Int. Immunopharmacol. 56 (2018) 330–338.
[23] X. Hu, H. Shen, Y. Wang, M. Zhao, Liver X receptor agonist TO901317 attenuates Paraquat-induced acute lung injury through inhibition of NF-kappaB and JNK/p38 MAPK signal pathways, Biomed. Res. Int. 2017 (2017) 4652695.
[24] J.M. Herter, J. Rossaint, T. Spieker, A. Zarbock, Adhesion molecules involved in neutrophil recruitment during sepsis-induced acute kidney injury, J. Innate Immun. 6 (2014) 597–606.
[25] T. Yasaka, K. Okudaira, H. Fujito, J. Matsumoto, I. Ohya, Y. Miyamoto, Further studies of lipid peroxidation in human paraquat poisoning, Arch. Intern. Med. 146 (1986) 681–685.
[26] G.P. Sykiotis, I.G. Habeos, A.V. Samuelson, D. Bohmann, The role of the antioxidant and longevity-promoting Nrf2 pathway in metabolic regulation, Curr. Opin. Clin. Nutr. Metab. Care 14 (2011) 41–48.
[27] Z. Liu, Y. Xiang, G. Sun, The KCTD family of proteins: structure, function, disease relevance, Cell Biosci. 3 (2013) 45.
[28] de Haan JB. Nrf2 activators as attractive therapeutics for diabetic nephropathy, Diabetes 60 (2011) 2683–2684.
[29] M. McMahon, D.J. Lamont, K.A. Beattie, J.D. Hayes, Keap1 perceives stress via three sensors for the endogenous signaling molecules nitric oxide, zinc, and alkenals, Proc. Natl. Acad. Sci. U. S. A. 107 (2010) 18838–18843.
[30] K.J. Kelly, W.W. Williams Jr., R.B. Colvin, S.M. Meehan, T.A. Springer, J.C. Gutierrez-Ramos, et al., Intercellular adhesion molecule-1-deficient mice are protected against ischemic renal injury, J. Clin. Invest. 97 (1996) 1056–1063.
[31] M. Mazzali, J.A. Jefferson, Z. Ni, N.D. Vaziri, R.J. Johnson, Microvascular and tubulointerstitial injury associated with chronic hypoxia-induced hypertension, Kidney Int. 63 (2003) 2088–2093.
[32] D.H. Kang, J. Kanellis, C. Hugo, L. Truong, S. Anderson, D. Kerjaschki, et al., Role of the microvascular endothelium in progressive renal disease, J. Am. Soc. Nephrol. 13 (2002) 806–816.
[33] H.R. Jang, H. Rabb, The innate immune response in ischemic acute kidney injury, Clin. Immunol. 130 (2009) 41–50.
[34] A.F. Bento, R.F. Claudino, R.C. Dutra, R. Marcon, J.B. Calixto, Omega-3 fatty acid-derived mediators 17(R)-hydroxy docosahexaenoic acid, aspirin-triggered resolvin D1 and resolvin D2 prevent experimental colitis in mice, J. Immunol. 187 (2011) 1957–1969.
[35] K. Ley, C. Laudanna, M.I. Cybulsky, S. Nourshargh, Getting to the site of inflammation: the leukocyte adhesion cascade updated, Nat. Rev. Immunol. 7 (2007) 678–689.
[36] J.F. Lima-Garcia, R.C. Dutra, K. da Silva, E.M. Motta, M.M. Campos, J.B. Calixto, The precursor of resolvin D series and aspirin-triggered resolvin D1 display anti-hyperalgesic properties in adjuvant-induced arthritis in rats, Br. J. Pharmacol. 164 (2011) 278–293.
[37] H. Hacker, M. Karin, Regulation and function of IKK and IKK-related kinases, Sci. STKE 2006 (2006) re13.
[38] B. Huang, X.D. Yang, A. Lamb, L.F. Chen, Posttranslational modifications of NF-kappaB: another layer of regulation for NF-kappaB signaling pathway, Cell. Signal. 22 (2010) 1282–1290.